

Phase transitions in $\text{Lu}_2\text{Ir}_3\text{Si}_5$: An experimental investigation by transport measurements

Y. K. Kuo and K. M. Sivakumar

Department of Physics, National Dong Hwa University, Hualien 97401, Taiwan

T. H. Su and C. S. Lue*

Department of Physics, National Cheng Kung University, Tainan 70101, Taiwan

(Received 11 February 2006; revised manuscript received 25 April 2006; published 18 July 2006)

We have investigated the coupled structural and electronic phase transition in the rare-earth ternary silicide $\text{Lu}_2\text{Ir}_3\text{Si}_5$ by means of electrical resistivity (ρ), Seebeck coefficient (S), as well as thermal conductivity (κ) measurements. Near the phase transition, pronounced anomalies in these transport properties with a significantly large hysteresis of about 40 K were noticed. By comparing the transition characteristics with the earlier reported charge-density-wave (CDW) systems $R_5\text{Ir}_4\text{Si}_{10}$ (R =rare-earth elements), our present investigation infers the possibility for the CDW transition accompanying a structural transition in this compound. In addition, possible mechanisms for the observed thermal hysteresis have also been proposed.

DOI: [10.1103/PhysRevB.74.045115](https://doi.org/10.1103/PhysRevB.74.045115)

PACS number(s): 71.45.Lr, 71.20.Eh, 65.40.-b

I. INTRODUCTION

The rare-earth transition-metal silicides and germanides with the general formula $R_5T_4X_{10}$ (R =rare-earth elements; T =transition elements, and X =Ge or Si) have attracted considerable attention due to the variety of phase transitions and remarkable physical properties they exhibit.¹⁻⁹ Superconductivity and charge-density-wave (CDW) formation, two entirely different cooperative phenomena, were found to coexist in these systems. Our earlier investigation on $\text{Lu}_5\text{Rh}_4\text{Si}_{10}$ and $\text{Lu}_5\text{Ir}_4\text{Si}_{10}$ have indicated anomalous features in the thermal and electrical transport properties around the charge-density-wave transitions.^{4,10,11} Unusual thermodynamic and structural behaviors have also been reported in the $R_2T_3X_5$ compounds.¹²⁻²² For example, a pronounced phase transition in $\text{Lu}_2\text{Ir}_3\text{Si}_5$ has been observed between 140 and 200 K (besides the superconductivity at around 3.5 K) by Singh *et al.*²³ from the specific heat measurement. Among the known $R_2T_3X_5$ alloys, only $\text{Lu}_2\text{Ir}_3\text{Si}_5$ shows such a transition at a substantially high temperature. Another case of $\text{Er}_2\text{Ir}_3\text{Si}_5$ also exhibits a weak anomaly at around 135 K. However, the anomalous feature could be only seen in the electrical resistivity.¹⁷

$\text{Lu}_2\text{Ir}_3\text{Si}_5$ crystallizes in an orthorhombic $\text{U}_2\text{Co}_3\text{Si}_5$ -type structure (space group *Ibam*) at room temperature. This material undergoes a structural transformation to another orthorhombic structure with a doubling of the unit cell at low temperatures.²³ A large drop in the magnetic susceptibility $\chi(T)$ and a sudden upturn in the electrical resistivity $\rho(T)$ across the structural transformation were found, revealing a substantial change in the Fermi-level density of states (DOS) during the transition. These findings suggest that the structural transformation is induced or accompanied by an electronic phase transition. The possibility of a magnetic origin of the phase transition has been excluded according to the magnetic field independence of the electrical resistivity.²³ In fact, many observed features of $\text{Lu}_2\text{Ir}_3\text{Si}_5$ (electronic/CDW transition coupled with a structural transition/doubling of the unit cell) have been found to be similar to those of $\text{Er}_5\text{Ir}_4\text{Si}_{10}$ and KC_{60} which have been connected to their electronic characteristics.

Typical signatures, a sudden decrease in magnetic susceptibility, a marked increase in electrical resistivity, and a large peak in specific heat, are usually associated with certain electronic phenomena such as the charge/spin density (CDW/SDW) waves or Jahn-Teller effect coupled with structural transition.^{26,27} However, the high- T transition in $\text{Lu}_2\text{Ir}_3\text{Si}_5$ is very distinct from those in other rare-earth ternary compounds.¹⁻⁹ Near the transition temperature, a significant thermal hysteresis (~ 40 K) and a broad transition width (~ 15 K) were reported.²³ Most remarkably, above the transition temperature the $\rho(T)$ curve measured upon cooling was found to be well below the one measured upon warming. To clarify this peculiar feature, we performed a detailed transport study by measuring the electrical resistivity, Seebeck coefficient, and thermal conductivity, especially in the vicinity of the transition. It is well known that the Seebeck coefficient measurement is very sensitive to the changes in the Fermi-level DOS, and thermal conductivity will yield valuable information on the role of lattice phonons during phase transitions. Our results indicate that the high- T phase transition is presumably due to a structural transition followed by a CDW transition. In addition, possible interpretations for the observed thermal hysteresis are also given.

II. EXPERIMENT

Polycrystalline $\text{Lu}_2\text{Ir}_3\text{Si}_5$ was prepared by arc-melting high-purity elements under argon atmosphere. To improve the homogeneity, the sample has been remelted several times under the identical preparation conditions. The resulting ingot was then sealed in a quartz ampoule with about 160 Torr of argon and annealed at 1250 °C for one day followed by three days at 1050 °C. Room-temperature x-ray diffraction (XRD) analysis taken with $\text{CuK}\alpha$ radiation confirms the expected orthorhombic $\text{U}_2\text{Co}_3\text{Si}_5$ -type structure with no traceable impurity phases. Electrical resistivity measurement was performed by a standard dc four-probe technique. Seebeck coefficient and thermal conductivity were simultaneously measured in a nitrogen/helium dewar using a direct heat

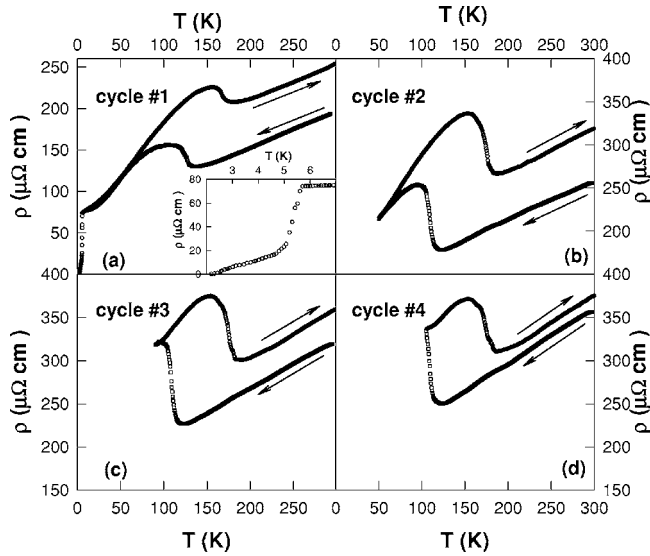


FIG. 1. Electrical resistivity as a function of temperature for $\text{Lu}_2\text{Ir}_3\text{Si}_5$ cycled at different temperature intervals. (a) 2–300 K, (b) 50–300 K, (c) 90–300 K, and (d) 105–300 K. A $\rho(T)$ plot around the superconducting transition temperature is displayed in the inset of (a).

pulse technique. Further details about the experimental techniques can be found elsewhere.⁴

III. RESULTS

A. Electrical resistivity

Figure 1 shows the result of T dependent $\rho(T)$ of $\text{Lu}_2\text{Ir}_3\text{Si}_5$ performed at various temperature intervals. In the inset of Fig. 1(a), a sharp drop at around 5.5 K, the onset temperature of superconducting transition, has been noticed. The superconducting transition temperature (T_C) of our sample is about 2 K higher than the value previously reported.²³ Upon raising temperature, a marked anomaly is seen between 120 and 200 K with a significant hysteresis between the cooling and warming data. The transition temperatures, determined from the minimum of $d\rho/dT$ vs T plot (not shown), are around 130 and 170 K for the cooling and warming runs, respectively. Such a feature indicates a first-order phase transition with a thermal hysteresis of about 40 K. Similar features have been reported in $\text{Lu}_5\text{Rh}_4\text{Si}_{10}$, attributed to the presence of metastable states arising from pinning of the CDW phase to the impurities.¹¹ However, the hysteresis behavior in $\text{Lu}_5\text{Rh}_4\text{Si}_{10}$ (of about 3 K) is much less pronounced than that of $\text{Lu}_2\text{Ir}_3\text{Si}_5$. It is worthwhile mentioning that the high- T transition temperature of our sample is about 40 K lower than that reported by Singh *et al.*, while our T_C is 2 K higher than their value.²³ We suspect that the differences are caused by the presence of disorder in our sample due to defects/inhomogeneities, which will be discussed in detail later.

Above and below the transition, the resistivity data exhibit metallic behavior, signifying that the electronic transition is a metal-metal transition as a result of partial gapping of the Fermi surface. The most remarkable feature of $\rho(T)$ is

that the warming curve lies above the cooling one and does not come down to merge together at high temperatures. Such behaviors have been noticed in the $\text{Gd}_5(\text{Si/Ge})_4$ system, which undergoes a first-order martensitic phase transition between 250 K and 300 K.²⁸ It has been suggested that the observed difference during thermal cycling in the electrical resistivity is due to the combination of phase transition itself and forming of microcracks in the sample volume. It is worth noting that the room-temperature (RT) electrical resistivity, $\rho(\text{RT})$, of $\text{Lu}_2\text{Ir}_3\text{Si}_5$ has been observed to decay with time after thermal cycling between 5 K and 300 K.²³ The decay of the electrical resistivity after being subjected to several thermal cycles seems to contradict the aspect of the electrical resistivity increasing due to the cracks developing in the samples, as the cracks would not anneal with time. We also notice that the electrical resistivity of $\text{Lu}_2\text{Ir}_3\text{Si}_5$ has returned back to its original value after six-month left in a room temperature since the first thermal cycle.

In the present work we have attempted to study this unusual thermal-history dependence by carrying out several cycles of $\rho(T)$ measurements with different temperature intervals. From Figs. 1(a)–1(d), we display a sequence of thermal cycles, where the sample was cooled down to 2 K (below the superconducting transition temperature), 50 K (well below the phase transition), 90 K (just below the phase transition), and 105 K (in the middle of the phase transition), respectively, and then heated up to room temperature. It is clearly seen that $\rho(T)$ of $\text{Lu}_2\text{Ir}_3\text{Si}_5$ depends strongly on thermal history with which the enhancement of room-temperature electrical resistivity decreases with increasing turning temperature (30% for cycle no. 1, 23% for cycle no. 2, 13% for cycle no. 3, and 5% for cycle no. 4, respectively). However, $\rho(T)$ would nicely match to each other during that particular thermal cycle as long as the sample stays above the phase transition. A subsequent thermal cycle down to 10 K renders again a nearly 30% difference in $\rho(\text{RT})$. These observations substantiate earlier conclusion that the microcracks cannot be accounted for the observed difference in $\rho(T)$ after thermal cycle,²³ and it should be related to the occurrence of the high- T phase transition.

Another interesting feature is that the observed step-like difference in $\rho(\text{RT})$ gradually decreases with a number of thermal cycles (cycling between 10 K and 300 K). We also noticed that while the thermal-history dependence of the transport properties is quite pronounced, heat capacity and magnetic susceptibility measurements show no such variations.^{23,28} It is likely that residual stresses, which may develop during cycling through the first-order structural phase transition, significantly affect the transport properties of $\text{Lu}_2\text{Ir}_3\text{Si}_5$, but have little or no effect on the thermodynamic characteristics.

B. Seebeck coefficient

A plot of Seebeck coefficient S versus temperature is shown in Fig. 2. With lowering temperature, S decreases quasilinearly, a typical character for nonmagnetic metals. In the normal state, the sign of S is positive, signifying that the hole-type carriers dominate the high- T thermoelectric trans-

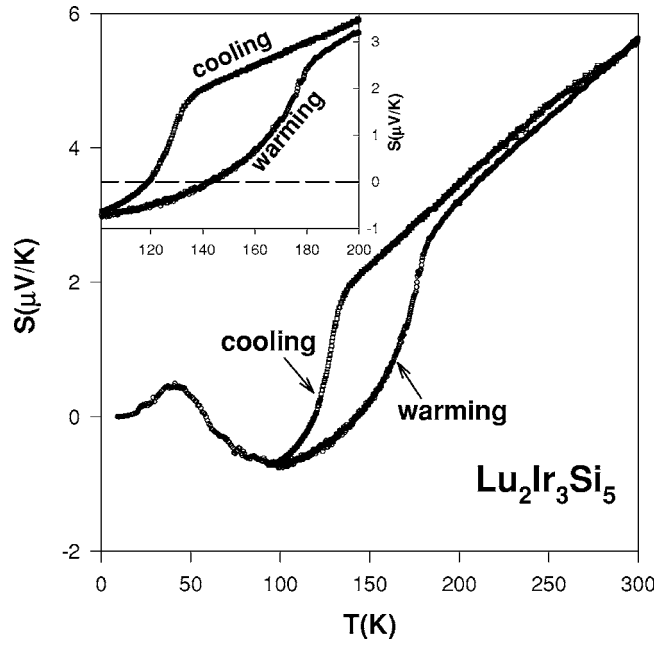


FIG. 2. Seebeck coefficient as a function of temperature for $\text{Lu}_2\text{Ir}_3\text{Si}_5$. The inset shows the details of thermal hysteresis near the transition.

port. Within the transition region, S drops rapidly and gradually changes its sign from positive to negative, indicative of a change of conduction mechanism or dominant carrier at the phase transition. Upon further cooling, S increases again and a broad maxima/peak appears around 40 K, ascribed to the phonon-drag effect. The phonon-drag effect and magnetic impurity scattering are generally active below 100 K, and is positive for the umklapp phonon-phonon scattering process. The onset of phonon-drag effect reverses the sign of S from negative to positive, leading to the appearance of a broad maximum. We notice that the characteristics of $S(T)$ in $\text{Lu}_2\text{Ir}_3\text{Si}_5$ are very similar to those in $\text{Lu}_5\text{Ir}_4\text{Si}_{10}$,⁴ in spite of the broader transition in the present case. Similar to that of the T -dependent electrical resistivity, a significant hysteresis of about 40 K in $S(T)$ is also seen. However the cooling and warming curves eventually match up at high temperatures in a given thermal cycle.

Since S varies rather linearly with temperature above the phase transition, indicating that diffusion Seebeck coefficient dominates the observed S in the high-temperature phase. Hence, one can extract the value of E_F through the classical formula $|S| = \frac{\pi^2 k_B^2 T}{2eE_F}$, assuming a one-band model with an energy-independent relaxation time. The value of $E_F = 1.5$ eV, obtained by fitting the data between 200 and 300 K, is in good agreement with the metallic nature of $\text{Lu}_2\text{Ir}_3\text{Si}_5$. It is known that the Seebeck coefficient measurement is a sensitive probe of energy relative to the Fermi surface, and the sign and magnitude of S strongly depend on the position of E_F in DOS. The positive value of S above the phase transition suggests the presence of lighter electron and heavier hole pockets in the energy band of $\text{Lu}_2\text{Ir}_3\text{Si}_5$. However, the electrons become heavier and thus dominate the thermoelectric transport below the phase transition. The

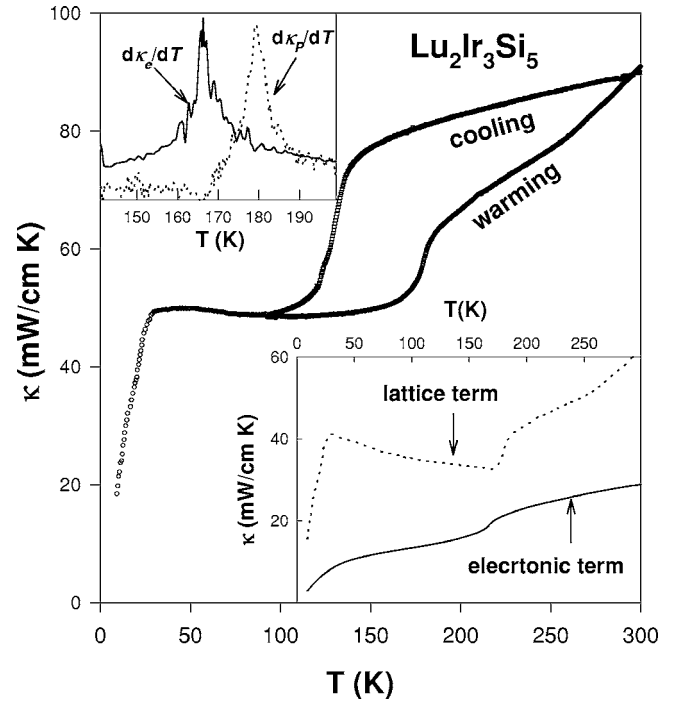


FIG. 3. Temperature dependence of the total thermal conductivity in $\text{Lu}_2\text{Ir}_3\text{Si}_5$. The insets show the calculated electronic (κ_e) and lattice (κ_p) thermal (bottom inset) and the $d\kappa/dT$ vs T plot near the transition for κ_e and κ_p (top inset). The analysis is taken with the warming processes of electrical resistivity and total thermal conductivity.

sharp decrease of S in the vicinity of phase transition is attributed to the rapid change of the band structure or DOS around E_F , associated with the electron-hole asymmetry. This would provide valuable information for the future band structure calculations on $\text{Lu}_2\text{Ir}_3\text{Si}_5$ and related compounds.

C. Thermal conductivity

The temperature-dependent thermal conductivity $\kappa(T)$ of $\text{Lu}_2\text{Ir}_3\text{Si}_5$ is displayed in Fig. 3. At low temperatures, κ increases with temperature and a broad maximum appears at around 40 K. This is a typical feature for the reduction of thermal scattering at lower temperatures in solids. As the temperature increases further, κ develops into a plateau and is nearly temperature independent. Near 180 K, a rapid jump in κ associated with the occurrence of a phase transition is clearly seen and above the phase transition, κ increases monotonically with increasing temperature. While the overall characteristics of $\kappa(T)$ in the present $\text{Lu}_2\text{Ir}_3\text{Si}_5$ are similar to $\text{Lu}_5\text{Ir}_4\text{Si}_{10}$ reported earlier,⁴ there are some noticeable differences between two systems near the phase transitions. First, the transition width is considerably wider in $\text{Lu}_2\text{Ir}_3\text{Si}_5$. Second, the well-defined peak observed in $\text{Lu}_5\text{Ir}_4\text{Si}_{10}$ around the transition temperature is absent in the present case. As a matter of fact, the presence of disorder or inhomogeneities in the sample could smear out the peak and thus broaden the transition. However, in the present study, the transition width is comparable or even sharper (see the top inset of Fig. 3) than the earlier report²³ and hence any major influence of

disorder/inhomogeneities on the measured thermal conductivity could be ruled out. Further, the most obvious difference, a significant thermal hysteresis loop near the phase transition between heating and cooling cycles in $\kappa(T)$ has been observed in $\text{Lu}_2\text{Ir}_3\text{Si}_5$.

Since the results of thermal conductivity provide valuable information about various scattering processes of thermal carriers, the present data would offer an opportunity to probe the interplay between the lattice and charge degrees of freedom in this compound. For conducting materials, the total thermal conductivity can be expressed as a sum of lattice (κ_P) and electronic (κ_e) thermal conductivities. The electronic contribution can be determined by means of the Wiedemann-Franz law, $\kappa_e\rho/T=L_0$, where ρ is the electrical resistivity and $L_0=2.45\times 10^{-8}\text{ W}\Omega\text{ K}^2$ the Lorenz number. As illustrated in the bottom inset of Fig. 3, the solid and dashed lines represent the calculated κ_e and κ_P for $\text{Lu}_2\text{Ir}_3\text{Si}_5$, respectively. Here the lattice thermal conductivity κ_P is obtained by subtracting the total thermal conductivity from the calculated electronic thermal conductivity κ_e . It is found that the electronic thermal conductivity constitutes about one quarter of the total thermal conductivity for $\text{Lu}_2\text{Ir}_3\text{Si}_5$, comparable to the previously investigated $R_5\text{Ir}_4\text{Si}_{10}$ ($R=\text{Y, Dy-Lu}$) compounds.^{2,4,9} It has been confirmed that the sharp drop in the total thermal conductivity near the CDW phase transition for the $R_5\text{Ir}_4\text{Si}_{10}$ system arises entirely from the reduction of electronic contributions. In the present case, the reduction in κ_e alone cannot account for the drop in the total thermal conductivity near the phase transition. Instead, the drop in κ_P is even larger and sharper than that of κ_e . Such an observation strongly suggests that the phonons play an important role for the high- T phase transition in $\text{Lu}_2\text{Ir}_3\text{Si}_5$. In addition, we noticed that the drop of κ_e occurs at the temperature about 15 K below that of κ_P , as shown in the inset of Fig. 3 (top). This is in contrast to the behavior in $R_5\text{Ir}_4\text{Si}_{10}$, where the sharp drop in the calculated and experimental thermal conductivity occurs almost at the same temperature.^{4,10} This finding indicates the possible coexistence of two phase transitions in $\text{Lu}_2\text{Ir}_3\text{Si}_5$, where the structural transition is followed by the electronic one. Definite conclusion for such a scenario needs further experimental support to differentiate these two types of transitions, nevertheless the drop in κ_P is significant in such a way that it clearly establishes the occurrence of a structural transition in $\text{Lu}_2\text{Ir}_3\text{Si}_5$.

IV. DISCUSSION

In this section we discuss the possible origin of the high- T phase transition observed in $\text{Lu}_2\text{Ir}_3\text{Si}_5$. The anomaly around the CDW transition in $\text{Lu}_5\text{Ir}_4\text{Si}_{10}$ has been ascribed to the opening of a gap over a portion of the Fermi surface. A substantial reduction in the DOS (36%) due to the gap opening has been reported from the specific heat and magnetic susceptibility data.¹ Similar to the case of $\text{Lu}_5\text{Ir}_4\text{Si}_{10}$, a large diamagnetic drop in the susceptibility and a well-defined peak in the specific heat were reported in $\text{Lu}_2\text{Ir}_3\text{Si}_5$. On these bases, the change in the electronic band structure, resulting in a DOS reduction due to partial gapping of Fermi surface during the phase transition has thus been proposed for this

material.²³ In fact, both the Jahn-Teller effect and CDW formation could lead to similar variations in the transport properties as a result of changes in the DOS. Another interesting aspect found in these classes of rare-earth transition-metal silicides is the interplay between the CDW and superconductivity. The competition between the superconductivity and CDW for the Fermi surface is well known in some of these compounds when they coexist. By suppressing/reducing the CDW transition temperature usually results in an enhancement of the superconducting temperature. For example, in the case of $\text{Lu}_5\text{Ir}_4(\text{Si}_{1-x}\text{Ge}_x)_{10}$ system, T_C increases (from 3 to 6 K) while T_{CDW} decreases (from 85 to 45 K) for low concentrations of Ge ($x=0.20$).^{3,13,23} In the present study, we noticed that the high- T phase transition is approximately 40 K lower than that of the earlier reported result,²³ while T_C is enhanced by 2 K. The intrinsic disorder in our sample may play the role of Ge substitution for Si as in the case of $\text{Lu}_5\text{Ir}_4(\text{Si}_{1-x}\text{Ge}_x)_{10}$. This finding further supports our claim that the high- T electronic transition is a CDW type. Therefore, the nature of this transition is most likely due to the formation of charge-density wave ground state accompanied by a first-order structural transition. As the temperature is lowered, the structural transition or doubling of the unit cell creates favorable conditions for the formation Fermi surface nesting/CDW. However, single crystal XRD measurements are still needed to clarify this scenario.

Now we turn our attention to the possible mechanism for the observed thermal hysteresis loop. The hysteresis features in the low-dimensional CDW materials are usually attributed to the pinning of the CDW phase to the impurities. For the present case of $\text{Lu}_2\text{Ir}_3\text{Si}_5$, as the material reaches the CDW ground state, the pinning forces are activated. In the warming process, if the pinned CDW try to retain its low temperature phase, then the cooperative interaction between the CDW phase (retained by pinning) and structural phase (with doubled unit cell) may lift the transition further to higher temperatures. Under these conditions, one should expect an extra hysteresis contribution in addition to the hysteresis due to the pinning of CDW, which could lead to a more pronounced hysteresis behavior as observed in $\text{Lu}_2\text{Ir}_3\text{Si}_5$.

It is worthy mentioning that a similar phase transition (coupled structural and CDW) has also been reported in $\text{Er}_5\text{Ir}_4\text{Si}_{10}$, which exhibits two CDW transitions.^{5,7} The low- T phase transition (60 K) was found to be first-order incommensurate-commensurate CDW transition while the high- T one (150 K) has been suggested as second-order due to the formation of normal-incommensurate CDW state. The presence of a low- T first-order transition may weaken the pinning force and hence no hysteresis could be seen for the high- T CDW transition. The unit cell doubling followed by the CDW formation has also been reported in the low dimensional material, KC_{60} . The ESR measurement has clearly shown the occurrence of electronic/CDW transition at a close interval of temperature just below the structural transition/doubling of the unit cell.^{24,25} With these respects, it would be very instructive to have similar investigations on the present $\text{Lu}_2\text{Ir}_3\text{Si}_5$ compound.

CONCLUSIONS

In conclusion, transport properties, including electrical resistivity, Seebeck coefficient, and thermal conductivity in

$\text{Lu}_2\text{Ir}_3\text{Si}_5$ have been studied in detail near the high- T phase transition. Anomalous features, sharp drops in the Seebeck coefficient and thermal conductivity and a sudden upturn in the electrical resistivity, in the vicinity of transition have been noticed. Analysis of thermal conductivity data suggests the possibility of two transitions in this material, most likely due to the structural transition followed by an electronic one. All these transport properties exhibit a pronounced thermal hysteretic behavior of about 40 K between the cooling (~ 140 K) and warming (~ 180 K) cycles. We associated this phenomenon with the cooperative interaction between the pinned CDW and low- T structural phase. The latter creates favorable conditions and thus lifts the coupled phase transi-

tion to higher temperatures upon warming. A strong similarity was observed for the present $\text{Lu}_2\text{Ir}_3\text{Si}_5$ and earlier investigated $\text{Lu}_5\text{Ir}_4\text{Si}_{10}$, pointing to a uniformity in the CDW characteristics. Single crystal XRD analysis and electronic band structure calculations are required for a better understanding of the unique phase transition found in $\text{Lu}_2\text{Ir}_3\text{Si}_5$.

ACKNOWLEDGMENT

The authors would like to thank the National Science Council of Taiwan for financially supporting this research under Contract Nos. NSC-94-2112-M-259-012 (Y.K.K.) and NSC-94-2112-M-006-001 (C.S.L.).

*Email address: cslue@mail.ncku.edu.tw

- ¹R. N. Shelton, L. S. Hausermann-Berg, P. Klavins, H. D. Yang, M. S. Anderson, and C. A. Swenson, *Phys. Rev. B* **34**, 4590 (1986).
- ²Y. K. Kuo, F. H. Hsu, H. H. Li, H. F. Huang, C. W. Huang, C. S. Lue, and H. D. Yang, *Phys. Rev. B* **67**, 195101 (2003).
- ³Yogesh Singh, R. Nirmala, S. Ramakrishnan, and S. K. Malik, *Phys. Rev. B* **72**, 045106 (2005).
- ⁴Y. K. Kuo, C. S. Lue, F. H. Hsu, H. H. Li, and H. D. Yang, *Phys. Rev. B* **64**, 125124 (2001).
- ⁵F. Gali, R. Feyerherm, R. W. A. Hendriks, E. Dudzik, G. J. Nieuwenhuys, S. Ramakrishnan, S. D. Brown, S. van Smaalen, and J. A. Mydosh, *J. Phys.: Condens. Matter* **14**, 5067 (2002).
- ⁶H. D. Yang, P. Klavins, and R. N. Shelton, *Phys. Rev. B* **43**, 7688 (1991).
- ⁷F. Gali, S. Ramakrishnan, R. Taniguchi, G. J. Nieuwenhuys, J. A. Mydosh, S. Geupel, J. Ludecke, and S. van Smaalen, *Phys. Rev. Lett.* **85**, 158 (2000).
- ⁸B. Becker, N. G. Patil, S. Ramakrishnan, A. A. Menovsky, G. J. Nieuwenhuys, and J. A. Mydosh, *Phys. Rev. B* **59**, 7266 (1999).
- ⁹Y. K. Kuo, Y. Y. Chen, L. M. Wang, and H. D. Yang, *Phys. Rev. B* **69**, 235114 (2004).
- ¹⁰C. S. Lue, F. H. Hsu, H. H. Li, H. D. Yang, and Y. K. Kuo, *Physica C* **364-365**, 243 (2001).
- ¹¹C. S. Lue, Y. K. Kuo, F. H. Hsu, H. H. Li, H. D. Yang, P. S. Fodor, and L. E. Wenger, *Phys. Rev. B* **66**, 033101 (2002).
- ¹²Yogesh Singh and S. Ramakrishnan, *Phys. Rev. B* **68**, 054419 (2003).
- ¹³Yogesh Singh and S. Ramakrishnan, *Phys. Rev. B* **69**, 174423 (2004).
- ¹⁴Yogesh Singh, S. Ramakrishnan, Z. Hossain, and C. Geibel, *Phys. Rev. B* **66**, 014415 (2002).
- ¹⁵N. G. Patil and S. Ramakrishnan, *Phys. Rev. B* **59**, 12054 (1999).
- ¹⁶Chandan Mazumdar, K. Ghosh, R. Nagarajan, S. Ramakrishnan, B. D. Padalia, and L. C. Gupta, *Phys. Rev. B* **59**, 4215 (1999).
- ¹⁷Yogesh Singh, D. Pal, and S. Ramakrishnan, *Phys. Rev. B* **70**, 064403 (2004).
- ¹⁸Z. Hossain, H. Ohmoto, K. Umeo, F. Iga, T. Suzuki, and T. Takabatake, *Phys. Rev. B* **60**, 10383 (1999).
- ¹⁹C. B. Vining, R. N. Shelton, H. F. Braun, and M. Pelizzone, *Phys. Rev. B* **27**, 2800 (1983).
- ²⁰H. F. Braun, *Phys. Lett.* **75A**, 386 (1980).
- ²¹J. A. Gotaas, J. W. Lynn, R. N. Shelton, P. Klavins, and H. F. Braun, *Phys. Rev. B* **36**, 7277 (1987).
- ²²C. B. Vining and R. N. Shelton, *Phys. Rev. B* **28**, 2732 (1983).
- ²³Yogesh Singh, Dilip Pal, and S. Ramakrishnan, A. M. Awasthi, and S. K. Malik, *Phys. Rev. B* **71**, 045109 (2005).
- ²⁴C. Coulon, A. Penicaud, R. Clerac, R. Moret, P. Launois, and J. Hone, *Phys. Rev. Lett.* **86**, 4346 (2001).
- ²⁵B. Verberck, A. V. Nikolaev, and K. H. Michel, *Phys. Rev. B* **66**, 165425 (2002).
- ²⁶Ivica Zerec, Alexander Yaresko, Peter Thalmeier, and Yuri Grin, *Phys. Rev. B* **66**, 045115 (2002).
- ²⁷K. Hamada, M. Wakata, N. Sugii, K. Matsuura, K. Kubo, and H. Yamauchi, *Phys. Rev. B* **48**, 6892 (1993).
- ²⁸E. M. Levin, A. O. Pecharsky, V. K. Pecharsky, and K. A. Gschneidner, *Phys. Rev. B* **63**, 064426 (2001).